

# EFFECTS OF DIFFERENT VENTILATION SPEEDS ON THE THERMAL ENVIRONMENT OF SOLAR GREENHOUSES

/

## 不同通风速度对日光温室热环境的影响

**Chuyuan ZHONG, Huiqun ZHOU**

Horsh (FUJIAN) Food Co., Ltd, FUJIAN, 363000, China

E-mail: z2019052798@163.com (Chuyuan Zhong)

Corresponding author: Huiqun Zhou

DOI: <https://doi.org/10.35633/inmateh-76-37>**Keywords:** Computational fluid dynamics, Solar greenhouse, Temperature, Ventilation rate

### ABSTRACT

The solar greenhouse is the main agricultural facility in northern China, providing a suitable environment for cultivating vegetables and flowers during the winter season. However, during the months of March and April, adjustments to the indoor temperature in northern Chinese solar greenhouses are necessary through the manipulation of upper and lower air vents. To investigate the impact of varying ventilation speeds on the thermal conditions within a solar greenhouse, Computational Fluid Dynamics (CFD) simulations were employed. The study assessed four different ventilation speeds on the air, soil, and wall temperatures within the greenhouse, assuming the absence of crops and disregarding humidity levels. The results showed that a wind speed of 0.5 m/s effectively reduced air temperature but had little effect on soil and wall temperatures; at wind speeds of 1.0 m/s and 1.5 m/s, the differences in air, soil, and wall temperatures inside the greenhouse were small. Considering economic benefits and crop growth conditions comprehensively, a wind speed of 1.0 m/s was identified as the optimal choice. This study provides data support and a theoretical basis for ventilation design in solar greenhouses.

### 摘要

日光温室是中国北方主要的农业设施，可为越冬期的蔬菜和花卉种植提供适宜环境。但是在中国北方 3 月和 4 月份需要通过开启上下风口调控室内温度。为研究不同通风风速对日光温室热环境变化影响，本文通过 CFD 模拟，在假定温室内无作物和忽略湿度工况下，设置 0 m/s、0.5 m/s、1.0 m/s、1.5 m/s 四种风速，研究其对温室内空气、土壤和墙体温度的影响。结果表明，0.5 m/s 风速可有效降低空气温度，但对土壤和墙体温度影响较小；1.0 m/s 和 1.5 m/s 风速下，温室内空气、土壤和墙体温度差异较小。综合考虑经济效益与作物生长环境等因素，1.0 m/s 风速为最佳选择。该研究为日光温室通风设计提供了数据支撑和理论依据。

### INTRODUCTION

Solar energy, as the best green and renewable energy source, is one of the effective ways to address energy shortages and environmental pollution through its maximum utilization (Liu W. et al., 2018). Agriculture, the most traditional industry utilizing solar energy, includes the Chinese solar greenhouse (CSG), a unique horticultural facility in northern China with thermal insulation walls on three sides and a plastic film on the south side, enabling off-season cultivation during the northern winter (Liu X. A. et al., 2022). However, current CSGs still suffer from excessively high daytime temperatures, leading to pest and disease outbreaks and reduced crop yields. Therefore, it is urgent to study the temperature and humidity in the crop area of CSGs to control the temperature within the range suitable for crop growth (Zhang Q. Y. et al., 2023).

Given the issue of high daytime temperatures in solar greenhouses causing pest damage and crop yield reduction, domestic scholars have made notable achievements in researching the thermal environment and optimizing ventilation in these greenhouses.

Lu L., (2022), designed and developed a ventilation control system for solar greenhouses, achieving automated regulation combined with sensor data and enhancing the intelligent level of the greenhouse environment. Yang Y. Q. et al., (2024), investigated the impact of different natural ventilation methods on the performance of solar greenhouses in desert areas, pointing out that rational ventilation design can effectively improve the greenhouse microclimate and promote crop growth.

Zhao G. M., (2024), focused on the impact of different natural ventilation methods on the environment of solar greenhouses and tomato growth. The experimental results indicated that the ventilation method directly affects the distribution of temperature and humidity in the greenhouse and the physiological state of crops.

With the development of Computational Fluid Dynamics (CFD) technology, many scholars have used CFD numerical simulation to study greenhouse ventilation. Several studies have investigated the indoor thermal conditions of solar greenhouses using Computational Fluid Dynamics (CFD) (Baglivo *et al.*, 2020; Dhiman *et al.*, 2019; Kim *et al.*, 2021; Wei *et al.*, 2022). The outcomes of these simulations offer valuable insights for optimizing the thermal regulation within solar greenhouse environments.

Wei D.D., (2022), systematically studied the numerical simulation of the thermal environment and ventilation characteristics of solar greenhouses, emphasizing the impact of wind speed and ventilation methods on the temperature field in the greenhouse.

Wu X.Y., (2022), conducted research on the structural optimization of energy-saving solar greenhouses based on CFD thermal environment simulation, proposing several structural improvement measures. Zhao Z., (2022), studied the summer cooling effect of a new type of connected solar greenhouses, verifying the practical value of CFD simulation in greenhouse design. Jing W. T., (2023), studied the ventilation simulation and optimization of active heat storage solar greenhouses, proposing ventilation control strategies based on heat storage characteristics. Zheng R.L., (2023), analyzed the impact of ventilation methods on greenhouse environment regulation through numerical simulation. Qiu Y., (2023), focused on the optimization and thermal environment analysis of pipeline ventilation in plant factories. Ding Y.Y., (2023), explored the experimental and numerical simulation methods of greenhouse thermal environment. Bo G.K., (2023), studied the growth response of greenhouse tomatoes under different ventilation modes and CFD environmental simulation. Zhou C.F., (2023), combined CFD simulation with fuzzy control system design to achieve intelligent control of the environment in edible fungus greenhouses, enhancing the stability of the greenhouse environment. Qu M.H., (2024), analyzed the temperature distribution characteristics in solar greenhouses through CFD numerical simulation. Mao C., (2024), focused on the heat transfer characteristics, combined with CFD simulation, to establish a greenhouse microclimate model and proposed model-based greenhouse environment control strategies. Qian C.H., (2024), combined CFD simulation with control system research to achieve precise control of the environmental temperature in agricultural greenhouses. Wan M. *et al.*, (2024), simulated the microclimate of solar greenhouses under different ventilation methods and analyzed the impact of crop transpiration on the humidity field in the greenhouse, emphasizing the coupling effect of ventilation and crop transpiration.

In summary, foreign scholars mainly focus on Venlo-type glass greenhouses and plastic greenhouses. This paper simulates the changes in indoor temperature and humidity fields in solar greenhouses under different ventilation types and speeds. The simulation provides references for natural ventilation control, making the greenhouse environment more suitable for crop growth, reducing pests and diseases, and improving economic benefits.

## MATERIALS AND METHODS

### ***The construction and meshing of the solar greenhouse geometric model***

Computational Fluid Dynamics (CFD) integrates mathematical models, fluid mechanics, and computer science to numerically simulate fluid flow, efficiently and intuitively solving complex fluid problems. It allows in-depth analysis of air flow and heat transfer in greenhouses. By simulating the impact of different wind speeds on the thermal environment of solar greenhouses, it reveals air flow patterns and temperature distribution changes. This provides a scientific basis for greenhouse ventilation design, energy-saving control, and crop growth environment optimization, holding significant theoretical and practical value.

A three-dimensional geometric model of a common solar greenhouse in Hulun Buir City, Inner Mongolia was constructed. The greenhouse faces south, with a span of 12 meters, a ridge height of 5 meters, a north wall height of 4.8 meters, and an east-west length of 100 meters. The north wall and the east-west gable are trapezoidal, with a base width of 8 meters and a top width of 2 meters. Solid Works software was used for 1:1 three-dimensional modeling, as shown in Figure 1.

In Computational Fluid Dynamics (CFD) simulation, fluent meshing aims to construct an accurate mathematical model. Mesh size and quality directly affect computational accuracy. For the solar greenhouse model, only the wall surface involving heat transfer needs to be refined. The 3D model uses structured, unstructured, and hybrid meshes.

Considering boundary refinement and accuracy, a hybrid mesh was chosen. The mesh size was set to 500 mm, with a total of 156,775 cells. Grid quality was determined using the grid metric, with values closer to 1 indicating better quality. The meshing and corresponding quality are illustrated in Figures 2 and 3.

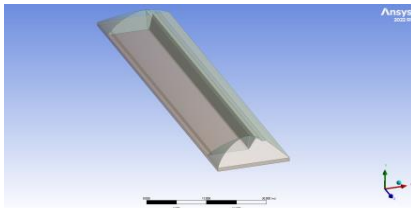


Fig. 1 - 3D model of solar greenhouse

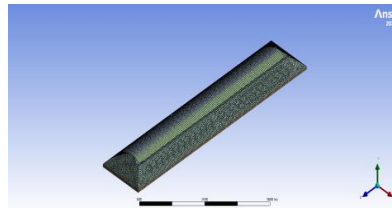


Fig. 2 - Mesh Division

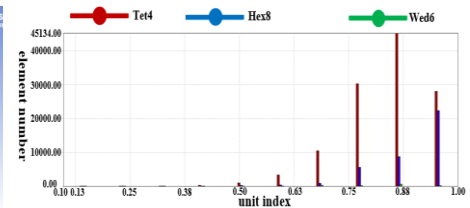


Fig. 3 - Grid Quality

### **The establishment of CFD numerical model**

#### **Model assumptions**

The temperature change in a solar greenhouse is a dynamic and complex process, influenced by various factors including greenhouse structure, outdoor climate, crop growth, and ventilation. To reduce analysis time and enhance accuracy, the CFD numerical model of greenhouse temperature was simplified as follows:

- (1) The solar greenhouse is in a completely closed state except for the upper and lower vents;
- (2) The influence of humidity on the temperature of the solar greenhouse was not considered;
- (3) The material parameters of each part did not change with the change of temperature.

#### **The basic control equation of CFD**

CFD is based on the conservation laws of mass, momentum, and energy for heat and mass transfer in fluids. The mass conservation equation describes the relationship between fluid motion and mass distribution. The momentum conservation equation links the rate of change of fluid momentum to external forces. The energy conservation equation is crucial in solar greenhouses, embodying the first law of thermodynamics and describing the conservation of total energy during fluid flow. Temperature changes and fluid motion interact to maintain energy balance.

#### **Turbulence model and Radiation model**

To better simulate the complex fluid flow and illumination environment inside the solar greenhouse and handle radiation heat transfer, this study selected the standard k- $\epsilon$  model, the DO radiation model, and the solar radiation model.

The solar radiation calculator sets the solar orientation, radiation intensity, and material thermal radiation parameters. The solar greenhouse is at 49°21'N, 119°25'E in the East 8 time zone. Solar radiation data from March 1, 2025 (sunny day) was used for simulation. Starting at 8:00, the coordinate axis was set with the X-axis positive to the north, the Z-axis positive to the east, the sunshine coefficient at 1, and illumination parameters configured using the solar calculator.

#### **Setting of material parameters**

Solar greenhouse experience temperature differences due to solar radiation during the day, causing minor changes in air density. The Boussinesq approximation, which treats air density as constant, simplifies the solution of fluid mechanics equations. The thermal properties of the greenhouse enclosure materials are shown in table 1.

#### **Boundary conditions and initial conditions**

The setting of boundary condition parameters has a great influence on the numerical simulation. According to the experimental data, the boundary conditions and initial conditions are determined as follows:

- (1) Setting of boundary conditions. The boundary conditions mainly include the setting of the boundary of the front and rear roofs, the east and west gables, the north wall and the soil of the solar greenhouse. The interface between the various parts is set to the coupling wall. From 8:00 a.m. to 15:00 p.m., the south roof was provided with a transparent plastic film.

(2) The setting of initial conditions. The exterior surface of the wall was set as a convective boundary condition with a heat transfer coefficient of 10; the south roof was set as a mixed (convective + radiative) boundary condition with a heat transfer coefficient of 15; the back roof was set as a convective boundary condition with a heat transfer coefficient of 5; the soil around was set as adiabatic. The experimental measurement data on March 6, 2025 were selected for model construction. The initial temperatures near the south, middle and wall of the greenhouse were 15.2°C, 16.8°C and 18°C, respectively. The outdoor temperature was applied to the outer surface of the greenhouse envelope. In addition, the initial values of the inner surface temperature of the north wall, soil and rear roof were 19°C, 20°C and 15°C, respectively.

(3) The upper and lower tuyeres were opened at the same time. The lower tuyere, measuring 100 m in length and 1 m in width, was located at the base of the southern shed film. In contrast, the upper tuyere, also 100 m long and 1 m wide, was positioned at the top of the shed film, approximately 1 m horizontally from the north wall and 5 m above the ground. The upper tuyere was set as the pressure outlet condition. The wind speed of the lower tuyere was set to 0m/s, 0.5m/s, 1m/s, and 1.5m/s. The effects of different wind speeds on air temperature, soil temperature, and wall temperature at different positions in the solar greenhouse were explored.

### Solve the setting of control parameters

In this simulation, the relaxation factors were set as follows: pressure at 0.3, density, body force, turbulent viscosity, and energy at 1,  $k$  and  $\epsilon$  at 0.8, and momentum at 0.7. The convergence criteria were set at  $1 \times 10^{-3}$  for continuity, momentum,  $k$ , and  $\epsilon$  equations, and at  $1 \times 10^{-6}$  for energy and radiation equations. These settings ensured high-precision results suitable for engineering applications.

Table 1

Material thermal property parameters of the solar greenhouse envelope

Parameters	PE	Wall	Soil	backward slope
Densities [kg/m <sup>3</sup> ]	950	2000	1600	70
Specific heat capacity [J/[kg·K]]	1600	1050	1050	1880
Thermal conductivity[W/[m·K]]	0.34	0.8	0.75	0.04
Absorption coefficient	0.15	0.88	0.88	0.1
Scattering coefficient	0	0.12	0.12	0
Index of refraction	1.72	1.92	1.92	1.72

## RESULTS AND DISCUSSION

In this research, CFD simulation was used to analyze the effects of four different wind speeds on the temperatures of air, soil, and walls inside a solar greenhouse across horizontal, vertical, and longitudinal dimensions. The coordinate origin was at the greenhouse's south bottom corner, with the y-axis extending upward and the x-axis pointing north.

### Influence of different ventilation rates on indoor air temperature

#### Influence of different ventilation rates on indoor air temperature along the horizontal direction

To investigate the impact of different wind speeds at the ventilation openings on air temperature at various horizontal positions in a solar greenhouse, a cross-sectional analysis along the north-south direction at the midspan in the east-west direction was conducted. Temperature variation curves at four different locations (Y=1200 mm, X=3000 mm, X=5000 mm, X=7000 mm, X=9000 mm) were selected for data analysis.

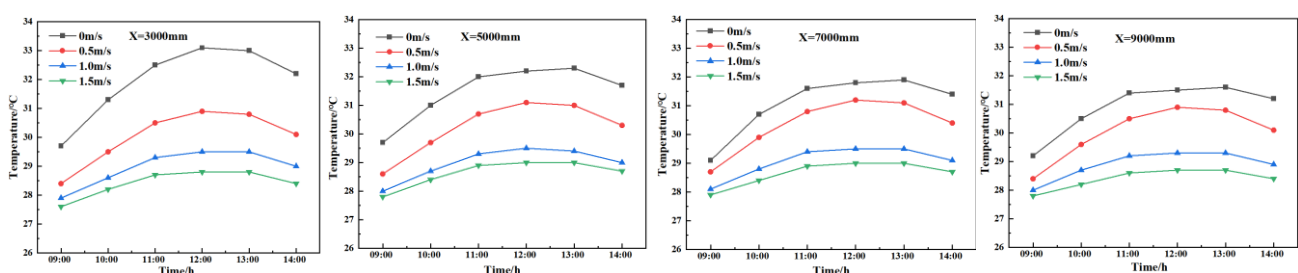


Fig. 4 - Influence of different wind speeds on indoor air temperature at various horizontal locations

As shown in Figure 4, under different wind speeds, the temperature at all horizontal measurement points increased rapidly from 9:00 to 11:00, stabilized from 11:00 to 13:00, and then decreased. Higher wind speeds led to lower temperatures, with the most evident differences at 13:00. At  $X=3000$  mm,  $X=5000$  mm,  $X=7000$  mm, and  $X=9000$  mm, the temperature differences between 0.5 m/s and 0 m/s wind speeds were  $2.2^{\circ}\text{C}$ ,  $1.3^{\circ}\text{C}$ ,  $0.8^{\circ}\text{C}$ , and  $0.8^{\circ}\text{C}$ , respectively. The differences between 1.0 m/s and 0.5 m/s were  $1.4^{\circ}\text{C}$ ,  $1.6^{\circ}\text{C}$ ,  $1.6^{\circ}\text{C}$ , and  $1.5^{\circ}\text{C}$ , respectively. The differences between 1.5 m/s and 1.0 m/s were  $0.7^{\circ}\text{C}$ ,  $0.4^{\circ}\text{C}$ ,  $0.5^{\circ}\text{C}$ , and  $0.6^{\circ}\text{C}$ , respectively.

It was concluded that Ventilation significantly reduces air temperature, with greater cooling effects at locations farther from the north wall. At 0.5 m/s, the cooling effect was more significant at  $X=3000$  mm; at 1.0 m/s, it was more pronounced at  $X=5000$  mm,  $X=7000$  mm, and  $X=9000$  mm.

### ***Influence of various ventilation rates on indoor air temperature in the vertical direction***

To investigate the influence of different wind speeds at the ventilation openings on air temperature at various vertical locations in a solar greenhouse, a cross-sectional analysis along the north-south direction at the midspan in the east-west direction was conducted. Temperature variation curves at four different locations ( $X=6000$  mm,  $Y=1000$  mm,  $Y=2000$  mm,  $Y=3000$  mm,  $Y=4000$  mm) were selected for data analysis.

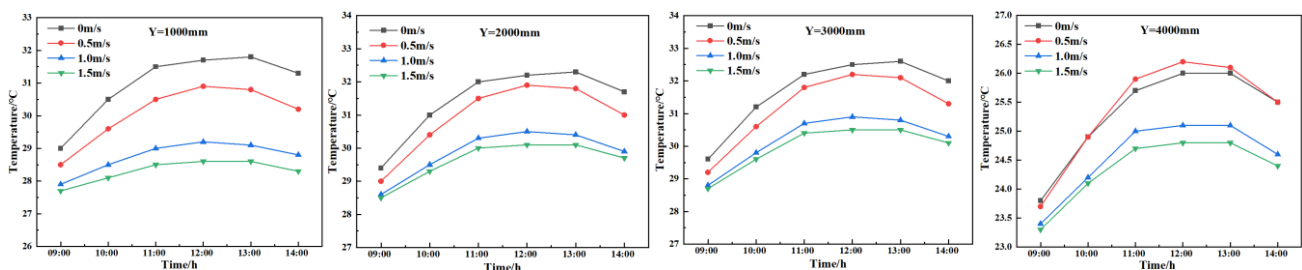


**Fig. 5 - Influence of different wind speeds on air temperature at various vertical locations**

As shown in Figure 5, under different wind speeds, the temperature trends at all vertical measurement points were consistent: rapid increase from 9:00 to 12:00, stabilization from 12:00 to 13:00, and gradual decrease after 13:00. Higher wind speeds led to lower temperatures. The temperature data at 0.5 m/s for the measurement point at  $Y=4000$  mm, located directly beneath the greenhouse film and influenced by unique convective effects, were excluded from the analysis. At 13:00, when temperature differences were most pronounced, the differences at  $Y=1000$  mm,  $Y=2000$  mm, and  $Y=3000$  mm were  $1.0^{\circ}\text{C}$ ,  $0.5^{\circ}\text{C}$ , and  $0.5^{\circ}\text{C}$  between 0.5 m/s and 0 m/s;  $1.7^{\circ}\text{C}$ ,  $1.4^{\circ}\text{C}$ , and  $1.3^{\circ}\text{C}$  between 1.0 m/s and 0.5 m/s; and  $0.6^{\circ}\text{C}$ ,  $0.3^{\circ}\text{C}$ , and  $0.3^{\circ}\text{C}$  between 1.5 m/s and 1.0 m/s.

It was concluded that ventilation significantly reduced air temperature at different vertical locations, with the effect diminishing as the  $Y$  value increased. A wind speed of 0.5 m/s had a more pronounced impact on the measurement point at  $Y=1000$  mm.

### ***Influence of different ventilation rates on indoor air temperature along the longitudinal direction***

To investigate the influence of different wind speeds at the ventilation openings on air temperature at various longitudinal locations in a solar greenhouse, temperature variation curves at four different locations ( $X=7000$  mm,  $Y=1200$  mm,  $Z=20440$  mm,  $Z=32940$  mm,  $Z=45440$  mm, and  $Z=70440$  mm) were analyzed.

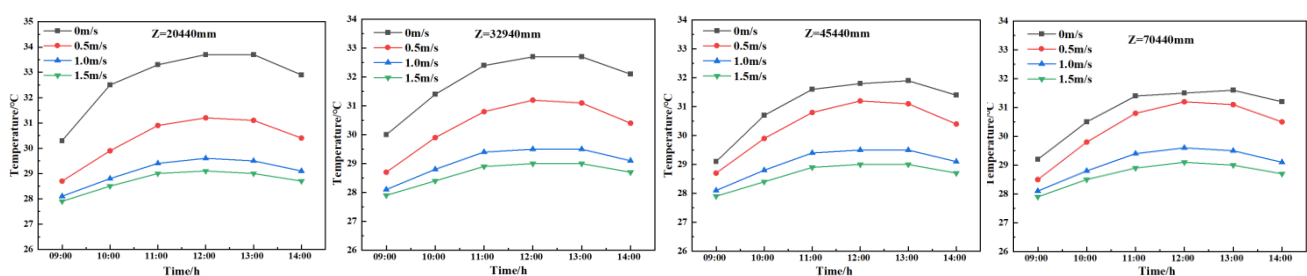


**Fig. 6 - Influence of different wind speeds on air temperature at various longitudinal locations**



As shown in Figure 6, under different wind speeds, the temperature trends at all longitudinal measurement points were consistent: rapid increase from 9:00 to 12:00, stabilization from 12:00 to 13:00, and gradual decrease after 13:00. The maximum temperature increases at the same measurement point varied significantly under different wind speeds: 3.5°C at 0 m/s, 2.7°C at 0.5 m/s, 1.4°C at 1.0 m/s, and 1.2°C at 1.5 m/s. This indicates that higher wind speeds result in smaller temperature increases and overall lower temperatures. At 13:00, temperature differences were most pronounced. At measurement points Z=20440 mm, Z=32940 mm, Z=45440 mm, and Z=70440 mm, the temperature differences between 0.5 m/s and 0 m/s were 2.6°C, 1.6°C, 0.8°C, and 0.5°C, respectively. The differences between 1.0 m/s and 0.5 m/s were all 1.6°C, and between 1.5 m/s and 1.0 m/s were all 0.5°C.

It was concluded that Ventilation significantly reduced air temperature at different longitudinal locations, with the effect diminishing from west to east. A wind speed of 0.5 m/s had a more pronounced impact at Z=20440 mm. Overall, ventilation effectively reduced air temperature, with 0.5 m/s and 1.0 m/s wind speeds having more pronounced cooling effects. However, considering the smaller influence range of 0.5 m/s compared to 1.0 m/s, and taking into account multiple factors such as economic benefits and crop growth environment, a wind speed of 1.0 m/s was determined to be a more optimal choice for ventilation.

### ***Influence of different ventilation rates on soil temperature***

#### ***Influence of different ventilation rates on soil temperature along the horizontal direction***

To investigate the influence of different wind speeds at the ventilation openings on soil temperature at various horizontal locations in a solar greenhouse, a cross-sectional analysis along the north-south direction at the midspan in the east-west direction was carried out. As documented in reference (Cheng W. W. et al., 2024), soil temperature at a depth of 50 mm from the ground surface is considerably influenced by air temperature. Thus, soil temperatures at a depth of 50 mm at locations X=3000 mm, X=5000 mm, X=7000 mm, and X=9000 mm were analyzed.

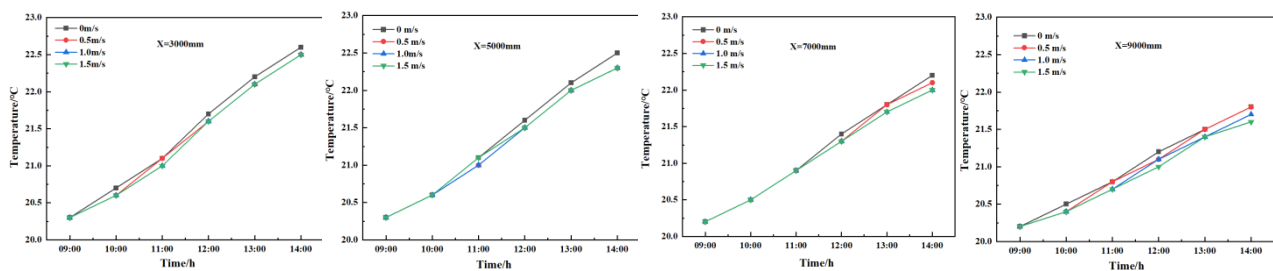


**Fig. 7 - Influence of different wind speeds on soil temperature at various horizontal locations**

As shown in Figure 7, from 9:00 to 14:00, the soil temperature at each location increased. Ventilation significantly affected soil temperature at different horizontal positions. After the ventilation openings were opened at 9:00, the soil temperatures at X=3000 mm and X=9000 mm changed rapidly, with clear temperature differences appearing soon after; the soil temperatures at X=5000 mm and X=7000 mm changed more slowly. Under various wind speeds, the soil temperature differences at each location grew over time, with maximum differences of 0.1°C, 0.2°C, 0.2°C, and 0.2°C, respectively.

At X=3000 mm and X=5000 mm, soil temperatures showed no significant variation under wind speeds of 0.5 m/s, 1.0 m/s, and 1.5 m/s, and were significantly lower than those at 0 m/s. At X=7000 mm and X=9000 mm, soil temperature decreased with increasing wind speed. The differences in soil temperature under wind speeds of 1.0 m/s and 1.5 m/s were minor, with maximum differences of 0°C and 0.1°C, respectively.

#### ***Influence of different ventilation rates on soil temperature along the vertical direction***

To investigate the impact of different wind speeds at the ventilation openings on soil temperature at various vertical locations in a solar greenhouse, a cross-sectional analysis along the north-south direction at the midspan in the east-west direction was conducted. Soil temperature variation curves at four different depths (50 mm, 200 mm, 350 mm, and 500 mm) at X=7000 mm were analyzed.

As shown in Figure 8, from 9:00 to 14:00, the soil temperature at each location increased progressively over time. Specifically, the rate of increase was faster from 9:00 to 11:00 and slower from 13:00 to 14:00.

After the ventilation openings were activated at 9:00, noticeable temperature differences at all locations under different wind speeds emerged by 11:00. The response rate was slower under a wind speed of 0.5 m/s compared to those under 1.0 m/s and 1.5 m/s.

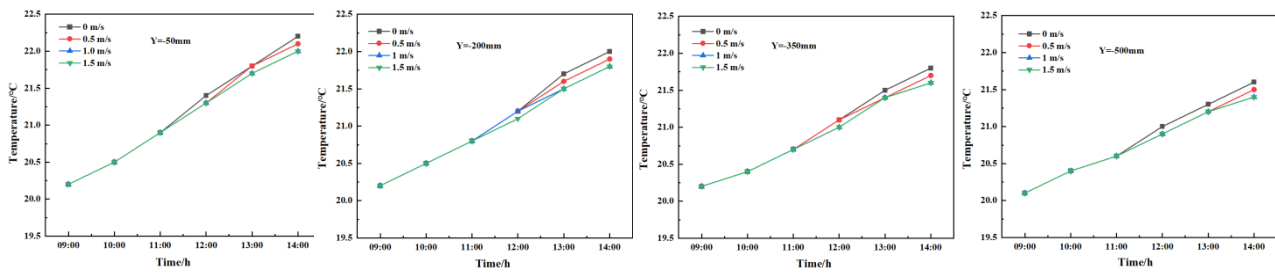


Fig. 8 - Influence of different wind speeds on soil temperature at various vertical locations

At depths of 50 mm, 200 mm, 350 mm, and 500 mm from the ground surface, opening the ventilation openings effectively reduced soil temperature. Under wind speeds of 1.0 m/s and 1.5 m/s, soil temperatures were similar and lower than at 0.5 m/s, with a maximum difference of 0.2°C.

#### ***Influence of different ventilation rates on soil temperature along the longitudinal direction***

To investigate the impact of different wind speeds at the ventilation openings on soil temperature at various longitudinal locations in a solar greenhouse, temperature variation curves at four different locations ( $X=7000$  mm, depth of 50 mm,  $Z=20440$  mm,  $Z=32940$  mm,  $Z=45440$  mm, and  $Z=57940$  mm) were analyzed.

As shown in Figure 9, from 9:00 to 14:00, the soil temperature at each location increased over time. Ventilation had a significant impact on soil temperature at different longitudinal positions. After the ventilation openings were activated, noticeable temperature differences emerged at  $Z=20440$  mm and  $Z=32940$  mm. For  $Z=45440$  mm and  $Z=57940$  mm, significant temperature differences appeared after 11:00. The soil temperature differences at each location under various wind speeds gradually widened over time, with the maximum differences reaching 0.3°C, 0.3°C, 0.2°C, and 0.1°C, respectively.

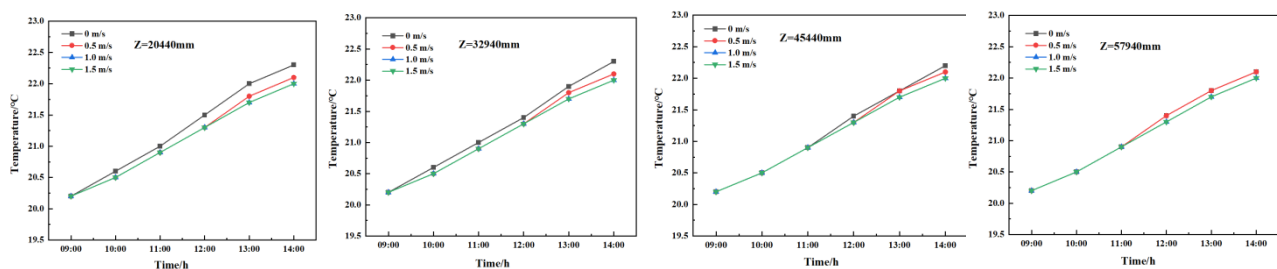


Fig. 9 - Influence of different wind speeds on soil temperature at various longitudinal locations

At locations  $Z=20440$  mm,  $Z=45440$  mm, and  $Z=32940$  mm, At  $Z=20440$  mm,  $Z=45440$  mm, and  $Z=32940$  mm, soil temperature was not affected by wind speeds of 0.5 m/s, 1.0 m/s, and 1.5 m/s during 9:00-12:00. From 12:00 to 14:00, soil temperatures under 1.0 m/s and 1.5 m/s were the same but significantly higher than those under 0.5 m/s, with a maximum difference of 0.1°C. At  $Z=57940$  mm, during 9:00-14:00, 0.5 m/s had no effect on soil temperature, matching that under 0 m/s. Soil temperatures under 1.0 m/s and 1.5 m/s were the same and significantly lower than that under 0.5 m/s, with a maximum difference of 0.1°C.

In summary, ventilation effectively reduced soil temperature. Wind speeds of 1.0 m/s and 1.5 m/s achieved more pronounced cooling effects on soil temperature. However, given that the impact of these two wind speeds on soil temperature was relatively close, and considering economic benefits and the crop growth environment, a wind speed of 1.0 m/s was selected for ventilation.

### ***Influence of different ventilation rates on wall temperature***

#### ***Influence of different ventilation rates on wall temperature along the horizontal direction***

To investigate the impact of different wind speeds on the horizontal variation of wall temperature in the greenhouse, a cross-sectional analysis along the north-south direction at the midspan of the east-west direction of the north wall was conducted. Temperature variation curves at four locations ( $L=300$  mm,  $L=600$  mm,  $L=900$  mm, and  $L=1200$  mm) from the inner side of the north wall were analyzed.

As shown in Figure 10, from 9:00 to 14:00, the wall temperature at locations  $L=300$  mm,  $L=600$  mm,  $L=900$  mm, and  $L=1200$  mm increased progressively over time. Different wind speeds had an impact on wall temperature at different horizontal positions. Specifically, at locations  $L=300$  mm and  $L=600$  mm, noticeable temperature differences emerged after 11:00. At locations  $L=900$  mm and  $L=1200$  mm, the temperature differences were consistent from 9:00 to 12:00 but began to change after 12:00. The wall temperature differences at each location under various wind speeds gradually widened over time, with the maximum differences reaching  $0.2^{\circ}\text{C}$ ,  $0.1^{\circ}\text{C}$ ,  $0.1^{\circ}\text{C}$ , and  $0.1^{\circ}\text{C}$ , respectively.

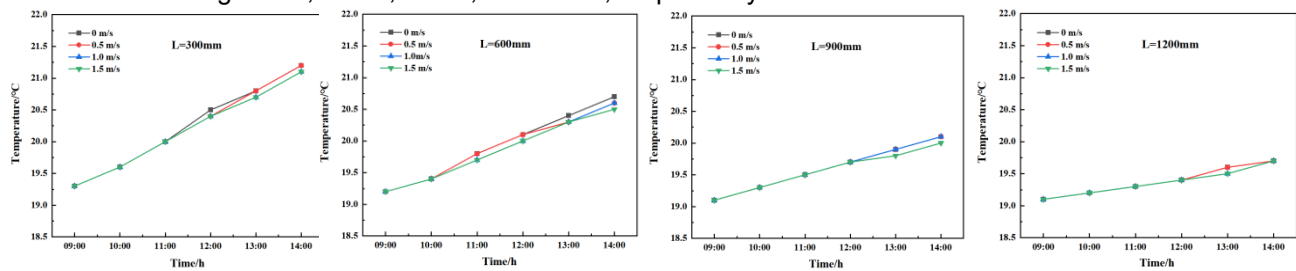


**Fig. 10 - Influence of different wind speeds on wall temperature at various horizontal locations**

At  $L=300$  mm and  $L=600$  mm, a  $0.5$  m/s wind speed had little impact on wall temperature, while  $1.0$  m/s and  $1.5$  m/s wind speeds effectively reduced it, with minimal differences (max  $0^{\circ}\text{C}$  and  $0.1^{\circ}\text{C}$ , respectively). At  $L=900$  mm,  $0.5$  m/s and  $1.0$  m/s had no effect, but  $1.5$  m/s significantly lowered wall temperature. At  $L=1200$  mm, all wind speeds had almost no impact.

#### ***Influence of different ventilation rates on wall temperature along the vertical direction***

To study the impact of different wind speeds on the vertical variation of wall temperature in the greenhouse, a cross-sectional analysis along the north-south direction at the midspan of the north wall was conducted, analyzing temperature variation curves at four locations ( $Y=1000$  mm,  $Y=1500$  mm,  $Y=2000$  mm, and  $Y=2500$  mm)  $200$  mm from the inner side of the north wall.

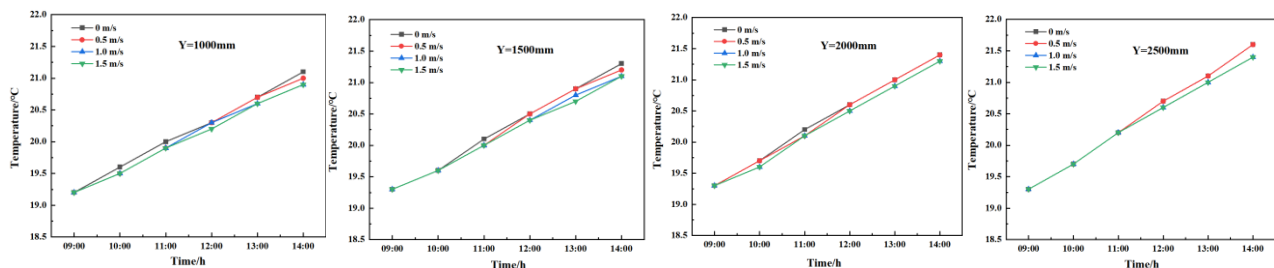


**Fig. 11 - Influence of different wind speeds on wall temperature at various vertical locations**

As shown in Figure 11, from 9:00 to 14:00, the wall temperature at various vertical locations increased over time. Different wind speeds had varying impacts on wall temperature. At  $Y=1000$  mm and  $Y=1500$  mm, the impact of wind speed showed synchronicity, with temperature differences gradually increasing over time. Differences were minimal from 9:00 to 11:00 but became more pronounced after 11:00. At  $Y=2000$  mm, the impact was slower, with stable differences from 9:00 to 11:00 and changes beginning after 12:00. At  $Y=2500$  mm, the impact was most delayed, with minimal differences from 9:00 to 12:00 and increasing differences after 12:00. The maximum temperature differences at each location under various wind speeds were  $0.2^{\circ}\text{C}$ ,  $0.2^{\circ}\text{C}$ ,  $0.2^{\circ}\text{C}$ , and  $0.2^{\circ}\text{C}$ , respectively.

At  $Y=1000$  mm,  $Y=1500$  mm,  $Y=2000$  mm, and  $Y=2500$  mm, wind speeds of  $1.0$  m/s and  $1.5$  m/s effectively reduced wall temperature with minimal differences between them. At  $Y=1000$  mm and  $Y=1500$  mm,  $0.5$  m/s had a smaller impact, while at  $Y=2000$  mm and  $Y=2500$  mm,  $0.5$  m/s had almost no effect.



### Influence of different ventilation rates on wall temperature along the longitudinal direction

To investigate the impact of different wind speeds on the longitudinal variation of wall temperature in the greenhouse, temperature variation curves at four different locations ( $X=10900$  mm,  $Y=1875$  mm,  $Z=20440$  mm,  $Z=32940$  mm,  $Z=45440$  mm, and  $Z=70440$  mm) were analyzed.

As shown in Figure 12, from 9:00 to 14:00, the wall temperature at  $Z=20440$  mm,  $Z=32940$  mm,  $Z=45440$  mm, and  $Z=70440$  mm increased. The impact of different wind speeds varied. At  $Z=20440$  mm, the wind speed effect was delayed, with differences increasing after 11:00. At  $Z=32940$  mm, wind speeds of 0.5 m/s, 1.0 m/s, and 1.5 m/s reduced wall temperature after 11:00. At  $Z=45440$  mm and  $Z=70440$  mm, the wind speed impact was synchronized, with differences increasing after 11:00, and wind speeds of 1.0 m/s and 1.5 m/s having a pronounced cooling effect. The wall temperature differences at each location gradually increased over time, with maximum differences of 0.4°C, 0.2°C, 0.2°C, and 0.1°C, respectively.

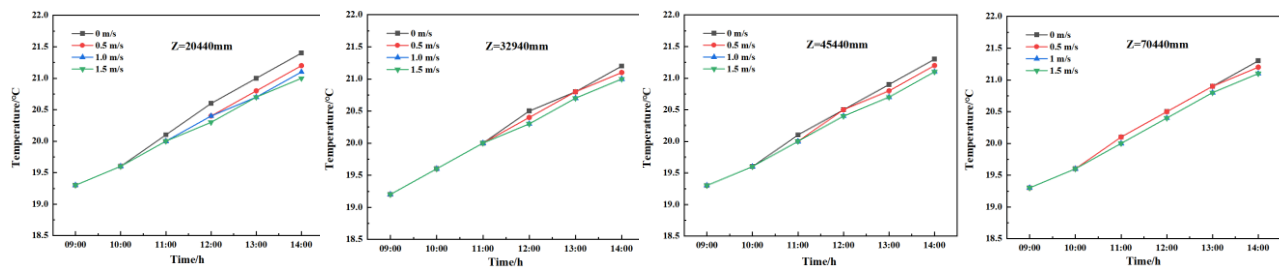


Fig. 12 - Influence of different wind speeds on wall temperature at various longitudinal locations

At a wind speed of 0.5 m/s, the impact on wall temperature was greatest at location  $Z=20440$  mm and smaller at locations  $Z=32940$  mm,  $Z=45440$  mm, and  $Z=70440$  mm. At location  $Z=20440$  mm, the difference in wall temperature between wind speeds of 1.0 m/s and 1.5 m/s was minimal, at 0.1°C. At locations  $Z=32940$  mm,  $Z=45440$  mm, and  $Z=70440$  mm, there were no significant differences in wall temperature between wind speeds of 1.0 m/s and 1.5 m/s.

The study found that greenhouse wall temperature rose over time, with varying impacts of wind speed by location. Horizontally, impact decreased with distance from the north wall. Vertically, higher positions showed more lag. Longitudinally, greater distance from the midspan increased lag. Wind speeds of 1.0 m/s and 1.5 m/s had stronger cooling effects than 0.5 m/s, with 1.5 m/s being more effective later on.

### CONCLUSIONS

Through CFD simulation of the solar greenhouse, the impact of different ventilation rates on the indoor air, soil, and wall temperatures within the solar greenhouse was investigated. The conclusions are as follows:

(1) Between 9:00 and 14:00, indoor air temperature initially increased rapidly, stabilized, and eventually decreased. Concurrently, soil and wall temperatures gradually increased over time. Additionally, wind speed inversely correlated with temperature, with higher speeds corresponding to lower temperatures.

(2) A wind speed of 0.5 m/s exerts minimal influence on indoor air temperature, soil temperature, and the temperature of the north wall. In contrast, wind speeds of 1.0 m/s and 1.5 m/s have a pronounced impact on these parameters. The magnitude of variation in indoor temperature, soil temperature, and north wall temperature was greater with an increase in wind speed from 0.5 m/s to 1.0 m/s compared to an increase from 1.0 m/s to 1.5 m/s.

In summary, a wind speed of 0.5 m/s effectively reduced indoor air temperature but had a minimal impact on soil and wall temperatures. The differences in temperature for indoor air, soil, and walls were relatively small under wind speeds of 1.0 m/s and 1.5 m/s.

### REFERENCES

- [1] Baglivo C., Mazzeo D., Panico S., Bonuso S., Matera N., Congedo P.M., Oliveti G. (2020). Complete greenhouse dynamic simulation tool to assess the crop thermal well-being and energy needs, *Appl. Therm. Eng.* 179.
- [2] Bo G.K. (2023). *Response of greenhouse tomatoes to different ventilation modes and CFD environment simulation research* (温室番茄对不同通风模式的响应及 CFD 环境模拟研究). North China University of Water Resources and Electric Power.

- [3] Cheng W. W., Wang C. C., Wang Y., Hao L. R., Liu Z. H., & Cui Q. L. (2024). Soil Marginal Effect and LSTM Model in Chinese Solar Greenhouse [J]. *Sensors*, 24(14):4730-4730.
- [4] Dhiman M., Sethi V.P., Singh B., Sharma A. (2019). CFD analysis of greenhouse heating using flue gas and hot water heat sink pipe networks, *Comput. Electron. Agric.*, 163.
- [5] Ding Y. Y. (2023). *Experimental and numerical simulation methods of greenhouse thermal environment* (日光温室热环境优化及相似模拟研究). North China Electric Power University (Beijing).
- [6] Jing W.T. (2023). *CFD simulation and optimization of active heat storage solar greenhouse ventilation* (基于 CFD 的主动蓄热日光温室通风模拟与优化). Northwest A&F University.
- [7] Kim R.W., Kim J.G., Lee I.B., Yeo U.H., Lee S.Y., Decano Valentin C. (2021) Development of three-dimensional visualisation technology of the aerodynamic environment in a greenhouse using CFD and VR technology, part 1: development of VR a database using CFD, *Biosyst. Eng.*, 207, 33–58.
- [8] Liu W., Liu L. Q., Guan C. G., Zhang F. X., Li M., Lv H., Yao P. J., & Ingenhoff J. (2018). A novel agricultural photovoltaic system based on solar spectrum separation [J]. *Sol Energy*, 162:84–94.
- [9] Liu X. A., Wu X. Y., Xia T. Y., Fan Z. L., Shi W. B., Li Y. M., & Li T. L. (2022). New insights of designing thermal insulation and heat storage of Chinese solar greenhouse in high latitudes and cold regions [J]. *Energy*, 242:122593.
- [10] Lu L. (2022). *Design and development of ventilation control system for solar greenhouses* (日光温室通风控制系统的设计与开发). Shenyang Agricultural University.
- [11] Mao C. (2024). *Analysis of heat transfer characteristics of greenhouse and modeling and control of greenhouse microclimate based on CFD* (基于 CFD 的温室传热特性分析及温室小气候建模与控制研究). Jiangxi University of Science and Technology.
- [12] Qiu Y. (2023). *Optimization and thermal environment analysis of pipeline ventilation in plant factories based on CFD* (基于 CFD 的植物工厂管道通风优化与热环境分析). Anhui Agricultural University.
- [13] Qu M. H. (2024). *Numerical simulation research on temperature environment of solar greenhouse based on CFD* (基于 CFD 的日光温室温度环境数值模拟研究). Shenyang Agricultural University.
- [14] Qian C. H. (2024). *CFD simulation and control system research of agricultural greenhouse environment temperature field* (农业大棚环境温度场 CFD 模拟及测控系统研究). Yancheng Institute of Technology.
- [15] Wei D.D. (2022). *Numerical simulation of thermal environment and ventilation characteristics of solar greenhouses* (日光温室热环境数值模拟与通风特性研究). Henan Agricultural University.
- [16] Wan M., Yang W., Liu Z. Q., Xu C. X., & Liu D. (2024). Simulation of microenvironment of solar greenhouse under different ventilation methods and research on crop transpiration (不同通风方式日光温室微环境模拟与作物蒸腾研究). *Transactions of the Chinese Society for Agricultural Machinery*, 55(01):328-338+349.
- [17] Wei D., Zhang Y., Liu S., Lv Y. (2022). Simulation study of ventilation characteristics of solar greenhouse under natural ventilation[J]. *Proceedings of the SPIE*, Volume 12160.
- [18] Wu X. Y. (2022). *Structural optimization of energy-saving solar greenhouses based on CFD thermal environment simulation* (基于 CFD 热环境仿真的节能日光温室结构优化研究). Shenyang Agricultural University.
- [19] Yang Y. Q., & Liu Y. F. (2024). The impact of different natural ventilation methods on the performance of solar greenhouses in desert areas (不同自然通风方式对沙漠日光温室性能的影响). *Agricultural and Technology*, 44(10):18-23.
- [20] Zhao G. M. (2024). The impact of different natural ventilation methods on the environment of solar greenhouses and tomato growth (不同自然通风方式对日光温室环境及番茄生长的影响). *China Agricultural Machinery Equipment*, (05):59-61.
- [21] Zheng R. L., Yang W., & Liu Z. Q. (2023). Numerical simulation of humidity and heat characteristics of solar greenhouses under different ventilation forms (不同通风形式日光温室湿热特性的数值模拟). *Journal of China Agricultural University*, 28(03):140-150.
- [22] Zhang Q. Y., & Du Z. Y. (2023). Numerical simulation of springtime temperature and humidity fields in the solar greenhouse based on soil evaporation and crop transpiration (基于土壤蒸发与作物蒸腾的春季日光温室室内温湿度场数值模拟). *Journal of Taiyuan University of Technology*, 1-14.
- [23] Zhou C. F. (2023). *CFD simulation and fuzzy control system design of edible fungus greenhouse environment* (食用菌温室环境 CFD 模拟与模糊控制系统设计). Huazhong Agricultural University.
- [24] Zhao Z. (2022). *Study on summer cooling effect of a new type of connected solar greenhouses based on CFD* (基于 CFD 的新型连栋日光能温室夏季降温效果研究). Nanjing Agricultural University.